CENTRAL ASIAN JOURNAL OF MEDICAL AND NATURAL SCIENCES

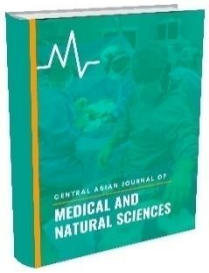

Volume: 04 Issue: 05 | Sep-Oct 2023 ISSN: 2660-4159

http://cajmns.centralasianstudies.org

Synthesis,Characterization and Study of the Molecular Docking With Biological Activity of Some Mannich Base Complexes Derived 4-Aminobenzoic Acid

1. **Ahmed Abd Khalaf**
2. **Afraa Saber Shihab**

Received 2nd Aug 2023,
Accepted 19th Sep 2023,
Online 21st Oct 2023

[1,2] Department of Chemistry / College of Education for Pure Sciences / Tikrit University

Abstract: This study involves the preparation of various organic compounds. Mannich base derivatives (A1, A2) were prepared by reacting 4-aminobenazoic acid with saccharin and benzaldehyde derivatives, using absolute ethanol as a solvent. Several complexes of Mannich bases (A3-A6) were obtained by reacting equimolar amounts of Mannich base derivatives (A1, A2) with the metal salt solution of cobalt and cadmium (MCln.XH2O), using ethanol as a solvent. The synthesized compounds and complexes were characterized using various spectroscopic techniques, including Fourier-Transform Infrared (FT-IR) spectroscopy, and Nuclear Magnetic Resonance (1H,13C-NMR) spectroscopy. Additionally, their melting points, purity, molar conductivity, and magnetic susceptibility were determined. The impact of some prepared compounds and complexes on the growth of two antibiotic-resistant bacterial strains, namely the Gram-negative Pseudomonas Aeruginosa and the Gram-positive Streptococcus Mutans, was studied. Amoxicillin, Ampicillin, and Ciprofloxacin were used as a control antibiotic. Some of the synthesized compounds exhibited significant inhibitory activity against the tested bacterial strains. Molecular docking studies were conducted for the compounds (A1, A2) against Pseudomonas Aeruginosa using the MOE software (2009). The energy minimization process was employed to achieve the most stable conformation (lowest energy barrier) for these compounds.

Key words: Saccharin, 4-Aminobezoic acid, Mannich Bases, Molecular Docking, Biological Activity.

1. Introduction

Saccharin, an artificial sweetener with a fascinating history, has found its way into our lives as a low-calorie alternative to sugar, revolutionizing the food and beverage industry [1]. This organic compound, which is around 300 times sweeter than sucrose [2], is renowned for its intense sweetness and its unique chemical properties [3]. Beyond its primary role as a sugar substitute [4], saccharin has also garnered significant attention in the field of chemistry for its ability to form complexes with various ions and molecules [5]. These saccharin complexes, a topic of growing interest in both academia and industry [6], offer a rich and diverse landscape of applications in fields ranging from pharmaceuticals to metallurgy. In this exploration [7], we will delve into the world of saccharin and its complexes [8], beginning with an overview of saccharin's discovery, properties [9], and sweetening power [10]. We will then venture into the realm of saccharin complexes, discussing the interactions between saccharin and various ions, metals, and organic molecules [11]. We will uncover how these complexes have been utilized in diverse applications, including drug delivery, catalysis [12], and the development of novel materials [13]. The intriguing chemistry and practical implications of saccharin complexes make them a compelling area of research, with the potential to influence multiple industries and improve our daily lives [14].

2. Experimental

2.1. Materials Employed:

All chemicals utilized in this study were procured from Fluka, Aldrich, and BDH Companies.

2.3. Preparation of Mannich Bases (A1, A2)

4-Aminobenzoic acid (0.003 mol, 0.366 g) dissolved in absolute ethanol (15 mL) was mixed with saccharin (0.003 mol, 0.549 g) dissolved in absolute ethanol (7 mL) and stirred for 30 minutes at a temperature of 50-60°C. Gradually, 0.003 mol of benzaldehyde derivatives dissolved in absolute ethanol (7 mL) were added dropwise. The mixture was then evaporated, resulting in the formation of a precipitate. This precipitate was recrystallized using absolute ethanol. Table (1) provides some physical properties of the Mannich base (A1, A2).

2.4. Preparation of Mannich Base Complexes (A3-A6)

To the solutions of Mannich base derivatives (A1, A2), dissolved in absolute ethanol (5 mL), the metal salt solutions of cobalt and cadmium ($MCln.XH_2O$) (0.28 mol, 0.28 mL) dissolved in absolute ethanol (3 mL) were added. The mixture was stirred for 3 hours at room temperature, then left to stand for an additional 2 hours. The solvent was evaporated, and the resulting precipitate was recrystallized using absolute ethanol. Table (1) outlines some physical properties of the prepared complexes.

2.5. Measurement of Biological Activity

Biological activity evaluation was performed through the Agar-well diffusion method. This involved inoculating the bacterial cultures across the entire growth medium using a cotton swab. Wells were then created in the agar medium employing a sterile puncture tool with a diameter of 6 mm. Subsequently, 100 microliters of each compound were placed within these wells on separate culture plates, each harboring a distinct bacterial strain. This process was replicated across all prepared solutions, encompassing their respective concentrations and targeted bacterial strains under study. The antibacterial activity assessment was conducted on two distinct bacterial types: the gram-positive Pseudomonas aeruginosa and the gram-negative Streptococcus mutans. To ensure the effectiveness of the test, both bacterial species were initially re-cultivated and subsequently incubated in a controlled laboratory environment at 37°C for a duration of 18-24 hours. This incubation period facilitated the

preparation of bacterial inoculums with a concentration of 1.5 x 10^8 bacterial cells per ml, calibrated against the McFarland standard set at an optical density of 0.5.

2.6. Molecular Docking Study of Some Prepared Compounds

Molecular docking studies were conducted for a selection of synthesized compounds (A_1, A_2) against a common bacterial strain, Escherichia coli, utilizing the MOE software (2009). The objective was to minimize the energy of the studied compounds (A_1, A_2) to attain the most stable conformation (lowest energy barrier). The protein structure of Escherichia coli was retrieved from the International Protein Bank, and high-performance computing resources were employed due to the demanding nature of these programs, which necessitate advanced, multi-core processors for efficient and expedited computational processes, particularly when dealing with large molecules and intricate atom arrangements, among other factors.

3. Results and Discussion

In this study, many compounds and complexes were prepared, as shown in Scheme (1).

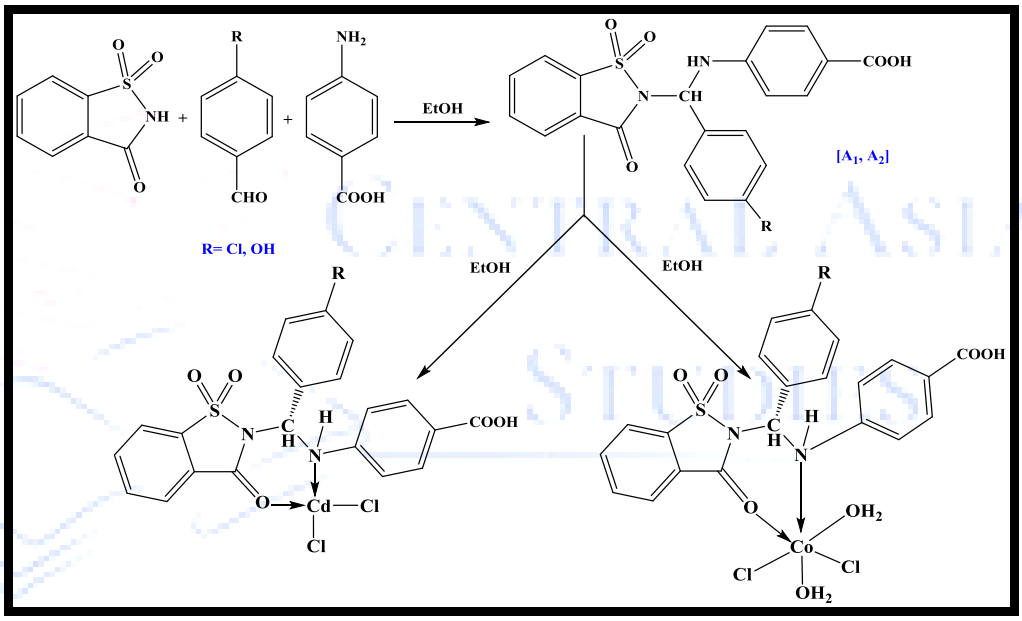

Scheme (1): Route of prepared compounds and complexes (A1-A6)

3.1. Characterization of Mannich Base Derivatives (A1, A2)

3.1.1. FT-IR Spectroscopy Analysis for Compounds (A1, A2)

In the study of the infrared spectrum of Mannich base derivatives (A9-A16), the emergence of absorption bands within the range of (3426-3450) cm^{-1} was observed, which can be attributed to the stretching vibrations of hydroxyl (OH) groups. Similarly, absorption bands in the range of (3194-3214) cm^{-1} were detected, corresponding to the stretching vibrations of amino (NH) groups. The appearance of absorption bands within the range of (3020-3052) cm^{-1} can be attributed to the aromatic carbon-hydrogen (CH) stretching vibrations. Additionally, absorption bands within the ranges of (2953-2975 and 2820-2870) cm^{-1} were noted, which are associated with aliphatic carbon-hydrogen (CH) stretching vibrations. Furthermore, a distinctive band within the range of (1724-1725) cm^{-1} was identified, originating from the carbonyl (C=O) group of carboxylic acids. Another band within the range of (1697-1706) cm^{-1} was attributed to the carbonyl (C=O) group of amides. Additionally, two absorption bands within the ranges of (1591-1604) cm^{-1} and (1477-1512) cm^{-1} were observed, indicating the presence of aromatic carbon-carbon (C=C) bonds. Furthermore, absorption bands within

the ranges of (1319-1327) cm^{-1} and (1150-1157) cm^{-1} were attributed to sulfur dioxide (SO_2) vibrations. These results, as presented in Table (2), closely aligned with the existing literature [15, 16].

3.1.2 ^{1}H-NMR Spectroscopy Analysis for Compounds (A1)

In the examination of the ^{1}H-NMR (Proton Nuclear Magnetic Resonance) spectrum of compound (A1), employing deuterated dimethyl sulfoxide (DMSO-d^6) as the solvent, several distinct signals were observed. A singular peak appeared at a chemical shift of 10.24 ppm, corresponding to a proton in two hydroxyl (OH) groups. In addition, multiple signals were detected within the range of 7.45-8.94 ppm, which could be attributed to protons in aromatic ring structures. Another singular peak emerged at a chemical shift of 7.31 ppm, indicating protons in two amino (NH) groups, while yet another singular peak at 6.69 ppm suggested protons in aliphatic (CH) groups. Furthermore, a signal at 2.59 ppm was noted, which could be ascribed to protons from the solvent, DMSO-d^6 [17, 18]. These findings are depicted in Figure (2).

3.1.3. ^{13}C-NMR Spectroscopy Analysis for Compounds (A1)

In the analysis of the ^{13}C-NMR spectrum of compound (A1), several notable signals were observed. A distinct peak appeared at a chemical shift of 167.57 ppm, corresponding to a carbon atom in the carbonyl (C=O) group of saccharin. Another signal emerged at a chemical shift of 161.37 ppm, attributed to a carbon atom in the carbonyl (C=O) group of carboxylic acids. Additionally, multiple signals were detected in the range of 125.28-140.58 ppm, indicating the presence of carbon atoms in aromatic ring structures. Another signal was observed at 121.60 ppm, associated with a carbon atom in aliphatic (CH) groups. Furthermore, signals in the range of 39.08-40.74 ppm were ascribed to carbon atoms from the solvent, DMSO-d^6, [19, 20]. These observations are illustrated in Figures (3).

3.2. Characterization of Mannich Base Complexes (A3-A6)

3.2.1. FT-IR Spectroscopy Analysis for Complexes (A3-A6)

During the study of the infrared spectrum of Mannich base complexes (A3-A6), several notable observations were made. A distinct reduction in the intensity of the (NH) band was observed within the range of 3160-3190 cm^{-1}. Additionally, a noticeable decrease in the intensity of the carbonyl (C=O) group in saccharin was observed in the range of 1666-1680 cm^{-1}. Moreover, new absorption bands were detected at around 923-968 cm^{-1}, corresponding to the stretching vibrations of (M-OH_2), and another new absorption band was identified within the range of 412-439 cm^{-1}, attributed to (νM-N). The remaining bands in the ligand maintained their respective wavenumbers, including an absorption band at 3296-3473 cm^{-1} attributed to hydroxyl (OH) stretching vibrations. Another band at 3038-3090 cm^{-1} was attributed to the aromatic carbon-hydrogen (CH) groups. Furthermore, two absorption bands in the ranges of (2917-2996 and 2809-2893) cm^{-1} were linked to aliphatic carbon-hydrogen (CH) groups. An additional band at 1722-1728 cm^{-1} was associated with the carbonyl (C=O) group of carboxylic acids. Furthermore, two new absorption bands were observed at (1575-1599 and 1480-1499) cm^{-1}, which can be attributed to aromatic carbon-carbon (C=C) bonds. Additionally, absorption bands were detected within the ranges of 1319-1386 cm-1 and 1125-1178 cm^{-1}, related to sulfur dioxide (SO_2) vibrations. A distinct absorption band at 751-770 cm^{-1} was attributed to carbon-chlorine (C-Cl) vibrations [21]. These findings are summarized in Table (2).

3.2.2. Measurement of Electrical Conductivity (Λ) and Molar Conductivity (Λm):

The electrical conductivity (Λ) of the prepared complexes was measured at a concentration of (10^{-3}) molar in a (DMSO) solution at a temperature of 25°C. After subtracting the solvent conductivity value, the equivalent conductance (Λ_{eq}) of the electrolyte can be defined as the conductance of a solution containing one gram equivalent of the electrolyte. The concentration (C) is expressed in units of ($eq.dm^{-3}$). The measurements indicated that all the prepared complexes exhibited conductivity values

ranging from (3-18) $ohm^{-1}.cm^{2}.mol^{-1}$, which represents a non-electrolyte solution [22]. Table (3) provides the results of molar conductivity measurements for the prepared complexes.

3.2.3. Magnetic Measurements of Prepared Complexes

The magnetic susceptibility of the prepared cobalt and cadmium complexes was calculated at a temperature of 25°C. The diamagnetic corrections (D) for the atoms in the organic molecules, metal ions, and non-organic radicals were applied using Pascal's constants for the constituent atoms of the prepared complexes. D (in $cm^{3}.molecule^{-1}$) is equal to the sum of the number of ions or atoms of the element multiplied by the Pascal's constant. The calculated values of the effective magnetic moment (μeff) for the prepared complexes were determined through magnetic measurements. The magnetic measurements of the prepared cobalt (II) complexes (A3, A5) revealed values ranging from 4.40 to 4.64 B.M. These results suggest that the cobalt (II) ion exhibits hexacoordination with a high-spin octahedral configuration [23, 24]. On the other hand, the cadmium complexes displayed diamagnetic characteristics.

3.3. Evaluation of the Biological Activity of Prepared Compounds and Complexes

In this study, the biological activity of prepared compounds and complexes was assessed against two types of bacteria: Streptococcus mutans and Pseudomonas aeruginosa using the well-diffusion method by measuring the inhibition zone. The results indicate that these compounds and complexes possess the ability to inhibit the growth of both Gram-positive and Gram-negative bacteria to varying extents. Amoxicillin, ampicillin, and ciprofloxacin. The prepared compounds and complexes exhibited good inhibitory effectiveness against Streptococcus mutans, with the highest inhibition zone of 30 mm. They also demonstrated good inhibitory effectiveness against Pseudomonas aeruginosa, with the highest inhibition zone of 31 mm. The concentration-inhibition relationship was inversely proportional, meaning that higher concentrations resulted in greater inhibition [25, 26], as shown in Table (5) and Figures (5).

3.4. Results of Molecular Docking Study for Some Prepared Compounds:

Molecular docking analysis of the prepared organic derivatives revealed the number and types of bonds formed with amino acid residues present at the active site. The study revealed that compound A_1 interacts with the remnants of amino acids present at the active site through the formation of two distinct types of bonds. There are four hydrogen bonds in total, with the first set connecting the amino acid residue ARG356, located at the active site, to the lone electron pair of the oxygen atom in the substituted phenol ring. The remaining three bonds connect the amino acid residues GLU112, HIS366, and ARG109, all present at the active site, to the lone electron pair of the oxygen atom in the carboxyl hydroxyl group. Moreover, two Pi-Alkyl bonds link the amino acid residues PRO111 and ARG256, also located at the active site, to the electron pairs of the aromatic ring. Similarly, the study showed that compound A_2 interacts with the amino acid residues found at the active site through the formation of two different types of bonds. There are four hydrogen bonds in total, with the first set connecting the amino acid residue ASP107, located at the active site, to the lone electron pair of the oxygen atom in the pentagonal ring sulfoxide group. The second set connects the amino acid residue ARG509, also at the active site, to the lone electron pair of the oxygen atom in the pentagonal ring carbonyl group. Additionally, the remaining two Pi-Alkyl bonds link the amino acid residues GLU112 and HIS375, present at the active site, to the electron pairs of the carboxyl hydroxyl group. Furthermore, one more Pi-Alkyl bond connects the amino acid residue ALA371, located at the active site, to the electron pairs of the aromatic ring.

Table (1): Physical Properties of Prepared Compounds and Complexes.

Comp. No.	R	Molecular formula	Color	M.p. °C	Y.%
A_1	Cl	$C_{21}H_{15}N_2O_5SCl$	White	196-198	75
A_2	OH	$C_{21}H_{16}N_2O_6S$	Yellow	185-186	81
A_3	Cl	$[Co(A_1)(H_2O)_2Cl_2]$	Light green	238-240	73
A_4	Cl	$[Cd(A_1)Cl_2]$	Brown	220-222	69
A_5	OH	$[Co(A_2)(H_2O)_2Cl_2]$	Light green	238-240	73
A_6	OH	$[Cd(A_2)Cl_2]$	Brown	220-222	69

Table (2): IR Absorption Results (cm^{-1}) for compounds and complexes (A1-A6).

Comp. No.	νOH νNH	ν(C-H) Arom.	ν(C-H) Aliph.	νC=O νC=O	ν(C=C) Arom.	ν(SO_2)	νC-Cl	νM-OH_2 νM-N
A_1	3450 3194	3020	2953 2820	1724 1697	1604 1477	1327 1157	709	-------
A_2	3426 3214	3052	2975 2870	1725 1706	1591 1512	1319 1150	-------	-------
A_3	3296 3169	3090	2974 2883	1722 1666	1583 1489	1340 1157	754	968 435
A_4	3451 3170	3073	2945 2809	1725 1670	1596 1480	1359 1162	765	923 412
A_5	3429 3188	3059	2996 2876	1723 1678	1575 1499	1386 1169	770	930 439
A_6	3420 3190	3040	2917 2841	1724 1680	1591 1480	1344 1125	752	956 432

Table (3): Molar Conductivity Measurements for the Prepared Complexes in DMSO.

No.	Complexes	Connectivity
A3	$[Co(A_1)(H_2O)_2Cl_2]$	15
A4	$[Cd(A_1)Cl_2]$	18
A5	$[Co(A_2)(H_2O)_2Cl_2]$	13
A6	$[Cd(A_2)Cl_2]$	17

Table (4): Magnetic Measurements for the Prepared Complexes at a Temperature of 25°C.

No.	Complexes	Amorous susceptibility $\chi g \times 10^{-6}$	Molar sensitivity $\chi M \times 10^{-6}$	Diamagnetic correction factor $D \times 10^{-6}$	Atomic sensitivity $\chi A \times 10^{-6}$	Effective magnetic torque μ_{eff} (BM)
A3	$[Co(A_1)(H_2O)_2Cl_2]$	15.23	8769.434	167.34	8936.774	4.64
A4	$[Co(A_2)(H_2O)_2Cl_2]$	13.5	7943.3	156.29	8099.59	4.40
A5	$[Cd(A_1)Cl_2]$	Dia	-	-	-	Square Planar
A6	$[Cd(A_2)Cl_2]$	Dia	-	-	-	Square Planar

Table (5): Biological effectiveness of prepared compounds, complexes and control parameters (in mm).

Comp. No.	*Streptococcus mutans*			*Pseudomonas aeruginosa*		
Conc. mg/ml	25	50	100	25	50	100
A_1	20	24	29	15	21	25
A_2	16	24	30	12	13	18
A_3	19	24	28	14	21	30
A_4	10	16	20	12	16	18
A_5	14	22	30	11	18	28
A_6	17	20	26	20	27	31
Amoxicillin	21	24	34	20	25	31
Ampicillin	23	26	32	21	26	32
Ciprofloxacin	20	27	33	19	25	30
Blank disk	0	0	0	0	0	0

Table (6): Values of binding energies for the prepared compounds

Comp. No.	RMSD	Docking Score
A_1	0.025	-8.9
A_2	0.035	-8.5

Figure (1): FT-IR spectrum of compound (A1)

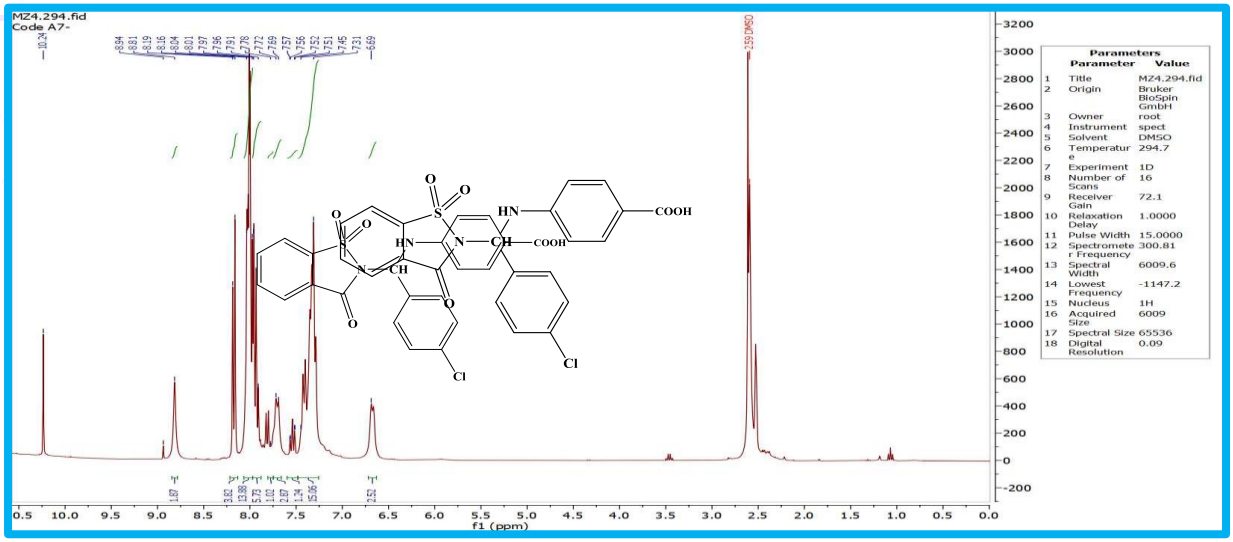

Figure (2): ^{1}H-NMR spectrum of (A1)

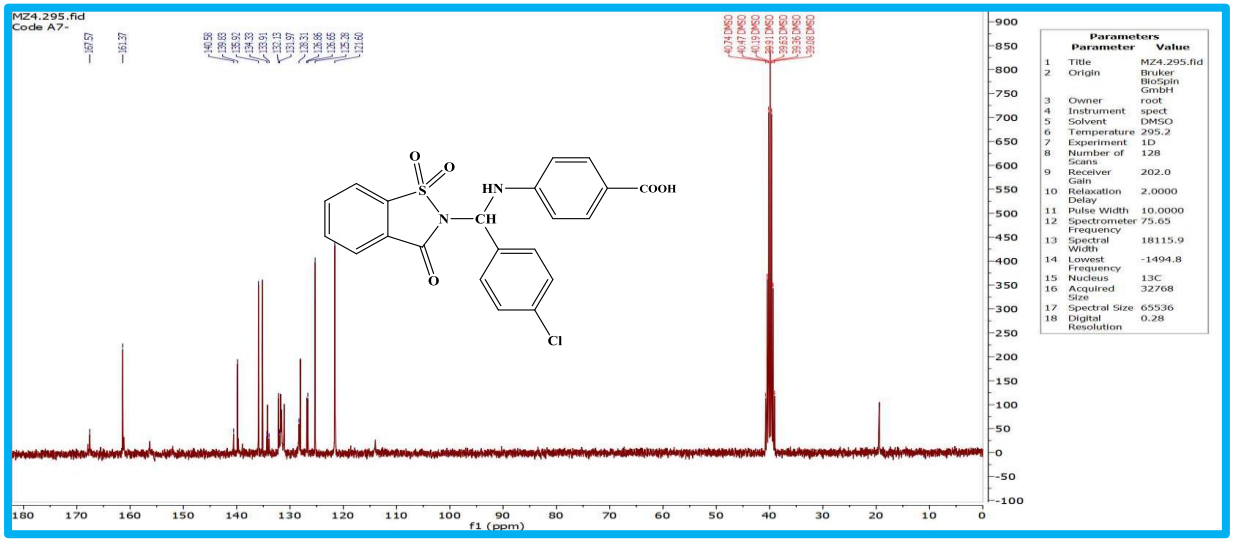

Figure (3): ^{13}C-NMR spectrum of (A1)

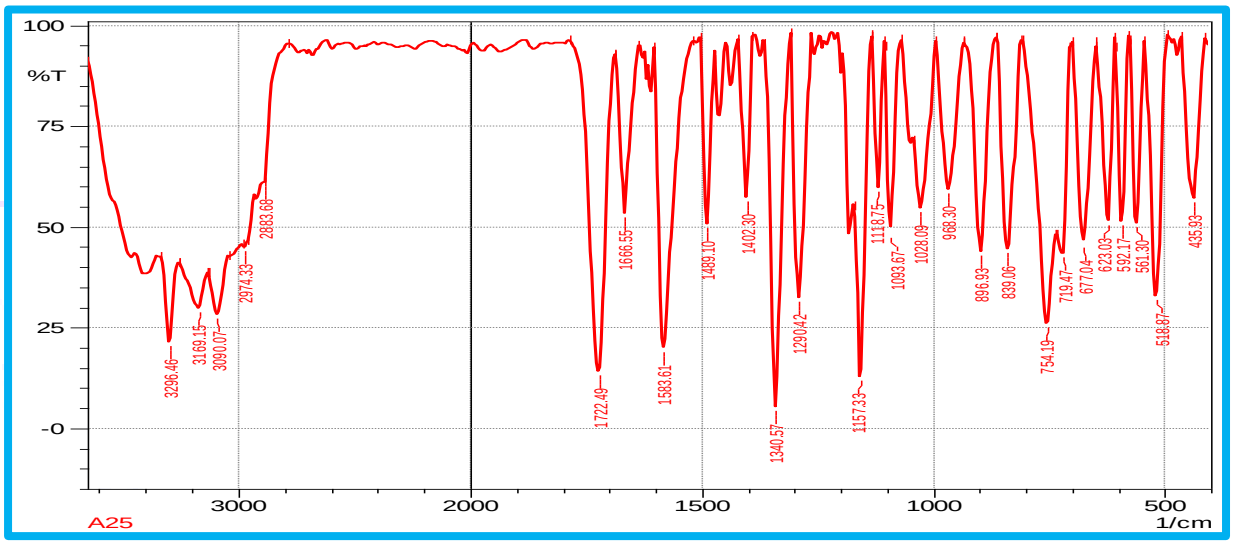

Figure (4): FT-IR spectrum of complex (A3)

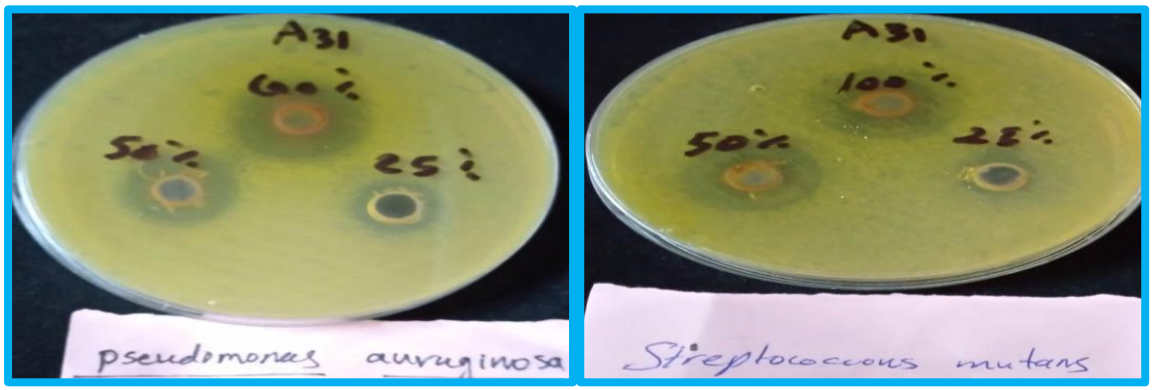

Figure (5): Inhibitory effectiveness of compound (A2) against both types of bacteria

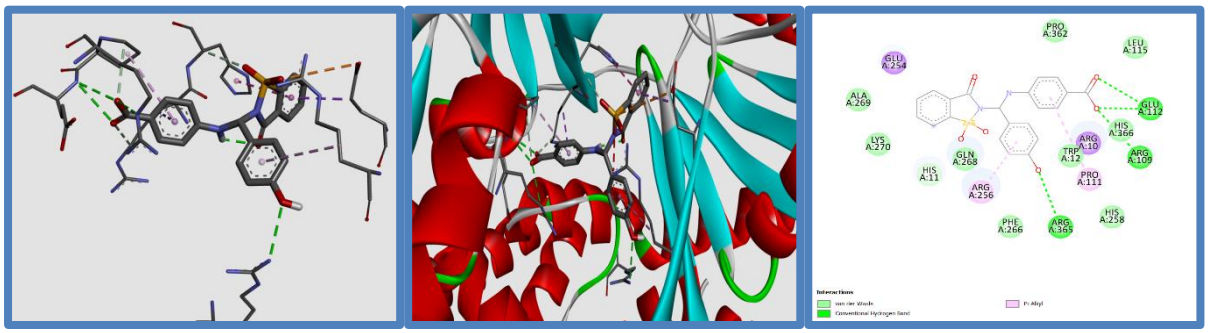

Figure (6): Interactions between compound (A1) in 3D and 2D dimensions

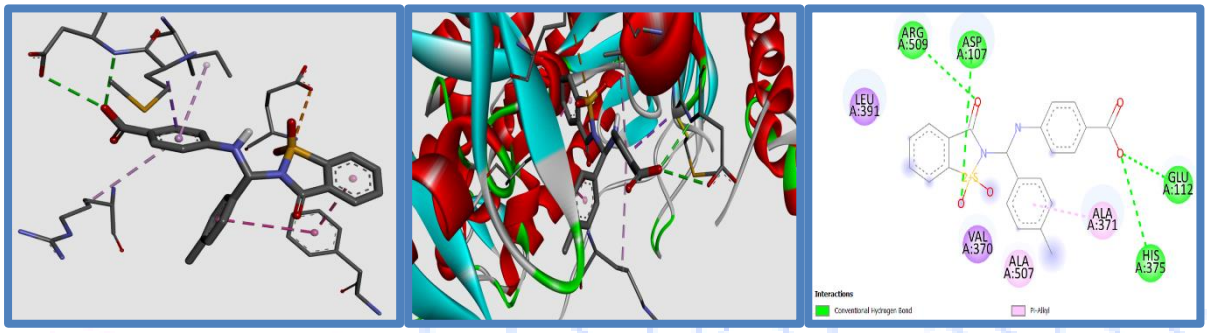

Figure (7): Interactions between compound (A2) in 3D and 2D dimensions

4. Conclusions: Derivatives of Mannich bases readily form complexes, especially with cobalt and cadmium metal salts. Cobalt complexes adopt an octahedral geometry in this study. Cadmium complexes exhibit a square planar geometry in this study. The prepared compounds and complexes displayed high stability and robustness, maintaining their structure, color, and melting point even with varying laboratory temperatures between winter and summer. The biological study revealed that most of the prepared compounds and complexes possess antibacterial activity and the ability to inhibit bacterial growth. These compounds exhibited higher biological efficacy compared to their parent compounds, which is of significant importance since the parent compounds are used as pharmaceuticals in the medical field.

5. Recommendations: Explore alternative preparation methods such as fusion, microwave-assisted synthesis, and ultrasound-assisted techniques, and compare them with the traditional method. Investigate the most stable conformational arrangements of the prepared compounds and complexes. Study the liquid crystalline properties of the prepared compounds and complexes. Evaluate the effect of the prepared compounds on different types of fungi, parasites, and pathogenic bacteria associated with human health, such as tuberculosis bacteria, which require specific media and environments for cultivation. Synthesize new complexes with elements like Pt, Zn, Ni, and Hg, particularly platinum, to investigate their effectiveness as anticancer agents. Investigate the possibility of attaching these ligands to natural polymers and their potential use as heavy metal ion removers from industrial water. Perform kinetic studies and calculate the thermodynamic functions of the prepared derivatives.

References

1. Ganiyu, S. O., de Araújo, M. J. G., de Araujo Costa, E. C., Santos, J. E. L., dos Santos, E. V., Martinez-Huitle, C. A., & Pergher, S. B. C. (2021). Design of highly efficient porous carbon foam cathode for electro-Fenton degradation of antimicrobial sulfanilamide. Applied Catalysis B: Environmental, 283, 119652.

2. Warner, D. J. (2008). Ira Remsen, saccharin, and the linear model. *Ambix*, *55*(1), 50-61.
3. Du, J., Xiao, G., Xi, Y., Zhu, X., Su, F., & Kim, S. H. (2020). Periodate activation with manganese oxides for sulfanilamide degradation. Water research, 169, 115278.
4. Dalaf, A. H. (2018). Synthesis and Characterization of Some Quartet and Quinary Hetero cyclic Rings Compounds by Traditional Method and Microwave Routes Method and Evaluation of Their Biological Activity. *M.Sc. Thesis, Tikrit University*, Tikrit, Iraq: 1-94 pp.
5. Dalaf, A. H., & Jumaa, F. H. (2018). Synthesis, Characterization of some 1,3-Oxazepane -4,7-Dione by Traditional and Microwave routes method and evaluation of their biological activity. *Al-utroha for Pure Science*. (8): 93-108.
6. Dalaf, A. H., Jumaa, F. H., & Jabbar, S. A. S. (2018). Synthesis and Characterization of some 2, 3-dihydroquinozoline and evaluation of their biological activity. *Tikrit Journal of Pure Science*, 23(8): 66-67.
7. Salwa, A. J., Ali, L. H., Adil, H. D., Hossam, S. A. (2020). Synthesis and Characterization of Azetidine and Oxazepine Compounds Using Ethyl-4-((4-Bromo Benzylidene) Amino) Benzoate as Precursor and Evalution of Their Biological Activity. *Journal of Education and Scientific Studies*, ISSN: 24134732. 16(5): 39-52.
8. Abd, I. Q., Ibrahim, H. I., Jirjes, H. M., & Dalaf, A. H. (2020). Synthesis and Identification of new compounds have Antioxidant activity Beta-carotene, from Natural Auxin Phenyl Acetic Acid. *Research Journal of Pharmacy and Technology*, 13(1): 40-46.
9. Muthukumar, R., Karnan, M., Elangovan, N., Karunanidhi, M., Sankarapandian, V., & Thomas, R. (2022). Synthesis, spectral, computational, wavefunction and molecular docking studies of 4-((thiophene-2-ylmethylene) amino) benzenesulfonamide from sulfanilamide and thiophene-2-carbalaldehyde. Journal of the Indian Chemical Society, 99(10), 100718.
10. Elangovan, N., Gangadharappa, B., Thomas, R., & Irfan, A. (2022). Synthesis of a versatile Schiff base 4-((2-hydroxy-3, 5-diiodobenzylidene) amino) benzenesulfonamide from 3, 5-diiodosalicylaldehyde and sulfanilamide, structure, electronic properties, biological activity prediction and experimental antimicrobial properties. Journal of Molecular Structure, 1250, 131700.
11. Greco, S. J., Lacerda, Valdemar, J., & Bezerra dos Santos, R. (2011). Recent Advances in the Asymmetric Catalytic Mannich Reaction. ChemInform, 42(52), no-no.
12. Skorbach, V., & Kurkina, Y. (2019). Influence of Medicinal Plant Extracts on the Number of Columns of Strain Escherichia Coli. indicators, 3, 6.
13. Hashem, H. E., Nath, A., & Kumer, A. (2022). Synthesis, molecular docking, molecular dynamic, quantum calculation, and antibacterial activity of new Schiff base-metal complexes. *Journal of Molecular Structure*, *1250*, 131915.
14. Salih, B. D., Dalaf, A. H., Alheety, M. A., Rashed, W. M., & Abdullah, I. Q. (2021). Biological activity and laser efficacy of new Co (II), Ni (II), Cu (II), Mn (II) and Zn (II) complexes with phthalic anhydride. *Materials Today: Proceedings*, 43, 869-874.
15. Aftan, M. M., Jabbar, M. Q., Dalaf, A. H., & Salih, H. K. (2021). Application of biological activity of oxazepine and 2-azetidinone compounds and study of their liquid crystalline behavior. *Materials Today: Proceedings*, 43, 2040-2050.

16. Aftan, M. M., Talloh, A. A., Dalaf, A. H., & Salih, H. K. (2021). Impact para position on rho value and rate constant and study of liquid crystalline behavior of azo compounds. *Materials Today: Proceedings*.

17. Aftan, M. M., Toma, M. A., Dalaf, A. H., Abdullah, E. Q., & Salih, H. K. (2021). Synthesis and Characterization of New Azo Dyes Based on Thiazole and Assess the Biological and Laser Efficacy for Them and Study their Dyeing Application. *Egyptian Journal of Chemistry*, 64(6), 2903-2911.

18. Khalaf, S. D., Ahmed, N. A. A. S., & Dalaf, A. H. (2021). Synthesis, characterization and biological evaluation (antifungal and antibacterial) of new derivatives of indole, benzotriazole and thioacetyl chloride. *Materials Today: Proceedings*. 47(17), 6201-6210.

19. Dalaf, A. H., Jumaa, F. H., & Salih, H. K. (2021). Preparation, Characterization, Biological Evaluation and Assess Laser Efficacy for New Derivatives of Imidazolidin-4-one. *International Research Journal of Multidisciplinary Technovation*, 3(4), 41-51.

20. Dalaf, A. H., Jumaa, F. H., & Salih, H. K. (2021). *MULTIDISCIPLINARY TECHNOVATION*. *Red*, *15*(A2), C44H36N10O8.

21. Dalaf, A. H., Jumaa, F. H., Aftana, M. M., Salih, H. K., & Abd, I. Q. (2022). Synthesis, Characterization, Biological Evaluation, and Assessment Laser Efficacy for New Derivatives of Tetrazole. In *Key Engineering Materials* (Vol. 911, pp. 33-39). Trans Tech Publications Ltd.

22. Alasadi, Y. Kh., Jumaa, F. H., Dalaf, A. H., Shawkat, S. M., & Mukhlif, M. Gh. (2022). Synthesis, Characterization, and Molecular Docking of New Tetrazole Derivatives as Promising Anticancer Agents. *Journal of Pharmaceutical Negative Results*. 13(3): 513-522.

23. Dalaf, A. H., Jumaa, F. H., & Yass, I. A. (2022, November). Synthesis, characterization, biological evaluation, molecular docking, assess laser efficacy, thermal performance and optical stability study for new derivatives of bis-1, 3-oxazepene and 1, 3-diazepine. In *AIP Conference Proceedings* (Vol. 2394, No. 1, p. 040037). AIP Publishing LLC.

24. Alasadi, Y. K., Jumaa, F. H., & Dalaf, A. H. (2022, November). Synthesis, identification, antibacterial activity and laser effect of new derivatives of bis-1, 3-oxazepene-4, 7-dione and 1, 3-diazepine-4, 7-dione. In *AIP Conference Proceedings* (Vol. 2394, No. 1, p. 040019). AIP Publishing LLC.

25. Dallakyan, S., & Olson, A. J. (2015). Small-molecule library screening by docking with PyRx. *Chemical biology: methods and protocols*, 243-250.

26. Fan, J., Fu, A., & Zhang, L. (2019). Progress in molecular docking. *Quantitative Biology*, *7*, 83-89.